Chapter 4

Halogen Bonding Assisted C-3 Benzylation of Indoles and *N*-Benzylation of Imidazoles at Room Temperature

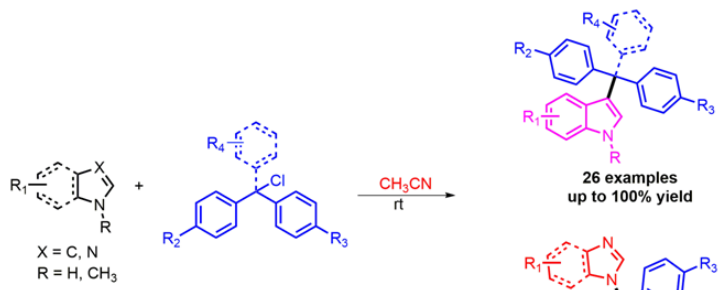

- ❑ C-Cl bond breaking through **halogen bonding**
- ❑ Catalyst-free benzylation
- ❑ Mild reaction conditions
- ❑ Broad substrate scope

Abstract: A study into the selective C-3 benzylation of indole and *N*-benzylation of imidazole derivatives using trityl chlorides is investigated experimentally under catalyst-free conditions at room temperature in acetonitrile. The Lewis basic nature of acetonitrile plays a significant role to carry out the reaction *via* halogen bonding by breaking down the C-Cl bond of the benzylating source. The UV-Vis and FT-IR analyses indicate the existence of halogen bonding which is the driving force of the reaction. This metal-free approach is suitable for a wide range of substrates, furnishing moderate to excellent yields (up to 100%) of benzylated products under ambient reaction conditions.

4.1 Introduction

Nitrogen-rich heterocycles (*N*-heterocycles) are significant structural motifs in organic synthesis and their site-selective benzylation at nitrogen atom or at carbon atom is very important from the medicinal and pharmaceutical chemistry viewpoint (Figure **4.1**) [1]. A large number of bioactive indole alkaloids are C-3 substituted and the formation of C-3 substituted products is mainly attributed to the high nucleophilicity of the carbon atom at that position [2,3]. The classical approach to the synthesis of C-3 benzylated indole is achieved by transition metal-catalyzed strategies [4], acid-catalyzed Friedel-Crafts-type reactions [5], and S_N2 type reactions [5]. However, these reported methodologies are not able to deal with the environmental issues and violate the sustainable developmental goals by using a stoichiometric amount of strong acids [5], expensive metal catalysts (Au, Pd, Pt, etc.), harsh reaction conditions, and the formation of unwanted by-products [6]. As a result, the development of mild and efficient reaction conditions to afford C-3 benzylated products is highly desirable in organic synthesis. Similar to indole, imidazole derivatives are integral scaffolds of various bioactive compounds, drugs, and agrochemicals [7]. *N*-benzylation of imidazoles represents a class of pharmaceutically active compounds [8] and also important synthetic intermediates in the preparation of different ionic liquids [9].

Different benzyl sources such as benzyl alcohols and benzyl halides are most commonly employed either for C-C or C-N bond formation in these *N*-heterocyclic molecules (Scheme **4.1**) [1]. Apart from these single aryl group containing benzyl sources, polyaryl agents like diphenyl methanol [4,5,10], triarylmethane chloride [6], etc. also play a significant role in the benzylation of *N*-heterocycles. Tri- and tetraarylmethanes are some well-known examples of polyaryl compounds as they attract researchers because of their rising importance in the field of material and medicinal chemistry. Triarylmethane derivatives are found to be active against tricomonads, helminthes, filariae, and their phenolic compounds exhibit antitumor and antioxidant properties [11]. The derivatives of triphenylmethane can provide stable quinoid structures which are common motifs of organic dyestuffs and fluorophores [12]. These derivatives are also utilized as protecting groups in organic synthesis to block different functional moieties transiently [12].

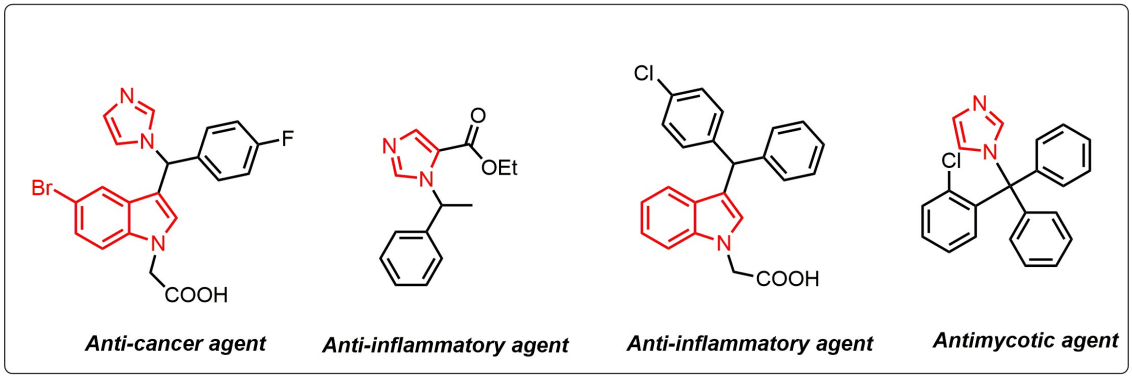

Figure **4.1**. Representative examples of pharmaceutically active *N*-heterocycles

In recent years, molecular interactions through halogen bonding have been illustrated experimentally by a large number of instances [13] and utilized as the driving force for different organic transformations [14]. Halogen bonding (XB) is a type of non-covalent interaction between a halogen atom (X) (halogen bond donor) and an electron donor atom (generally Lewis base, halogen bond acceptor) (Figure **4.2**) [15]. In this non-covalent interaction, the area directly utilized in bonding is the electropositive region generated at the outermost portion of the halogen atom which is projected away from the covalent bond [15]. The electropositive region is termed as the sigma hole (σ-hole), which is the localized deficient of electrical charge opposite to σ-bond [13]. The other area is the electronegative belt appears perpendicular to the covalent bond concerning the halogen atom. As a result, an electronic gradient is developed on the surface of the halogen atom, moving from outermost portion (electropositive region) to the equator (electronegative region). The electronic distribution highlights distinct regions (positive and negative) that offer the characteristic directional nature of halogen bond. A recent report by Jin group established that chloromethane could interact with various Lewis basic nitrogen sites (CCl_3CN, CH_3CN, FCN, ClCN, BrCN, SiH_3CN, etc.) through halogen bonding [16]. Since acetonitrile (CH_3CN) acts as Lewis basic halogen bond acceptor site, it can offer this type of bonding with polyaryl benzyl source such as trityl chloride and thereby triggering the benzylation of *N*-heterocyles. As compared to covalent force, this type of non-covalent interaction is dominant in biological functions because of its lesser rigidity [17]. Halogen bonding is found in ligand-to-metal binding, folding of molecules, hormone recognition by receptors, drug designing, crystal engineering, and organic synthesis [18].

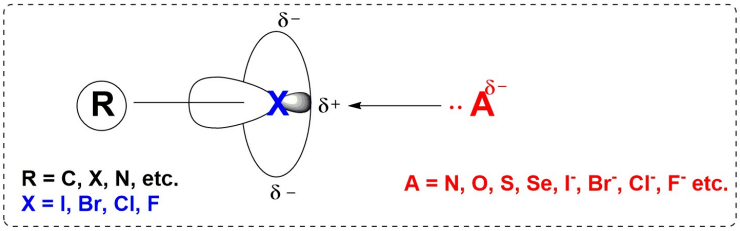

Figure **4.2**. Schematic representation of interaction in halogen bonding

In this context, we have carried out C-3 benzylation of indoles and *N*-benzylation of imidazoles using trityl chloride in CH_3CN at room temperature through halogen bonding under catalyst-free conditions (Scheme **4.1**).

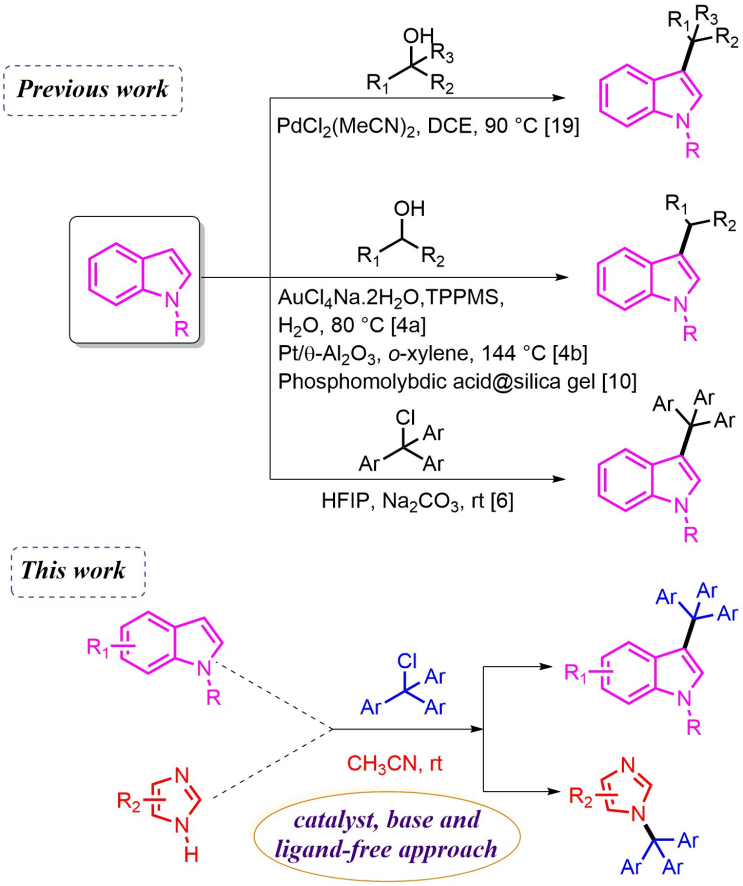

Scheme **4.1**. C-C and C-N bond formation *via* halogen bonding

4.2 Experimental Section

4.2.1 General procedure for the synthesis of C-3 benzylated indoles

A mixture of indole (0.5 mmol), trityl chloride (0.5 mmol), and CH_3CN (2 mL) was taken in a 50 mL round-bottomed flask. The reaction mixture was stirred at room temperature (27 °C) for the appropriate time. The completion of the reaction was observed by TLC and the reaction mixture was then extracted with ethyl acetate, washed with brine solution, and dried over with anhydrous sodium sulfate. To acquire the desired product, column chromatography was done using silica gel and hexane:ethyl acetate as solvent system.

4.3 Results and Discussion

4.3.1 Optimization of reaction conditions

To explore the catalytic efficiency of halogen bonding triggered by Lewis basic nature of CH_3CN, *N*-methylindole, and trityl chloride were used as model substrates and the optimization is displayed in Table **4.1**.

Table **4.1**. Screening of reaction conditions[a]

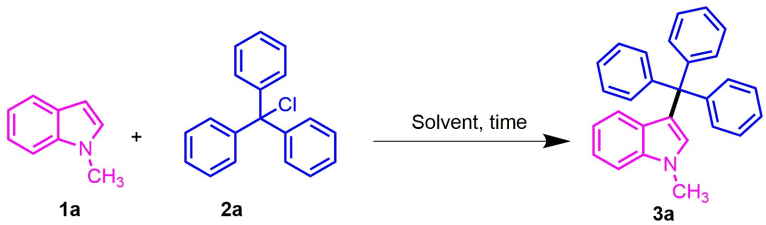

Entry	Solvent (mL)	Time (h)	Yield (%)[b]
1[c]	CH_3CN	2	100
2	**CH_3CN**	**2**	**100**
3	EtOH	24	27
4	*i*PrOH	24	12
5	MeOH	24	40
6	Toluene	24	43
7	H_2O	24	NR
8	DMSO	24	NR
9	DMF	24	NR
10	THF	24	NR
11[d]	CH_3CN	24	54

[a]Reaction conditions: **1a** (1 equiv.), **2a** (1 equiv.), Solvent (2 mL), rt, [b]Isolated yields, [c]at 50 °C, [d]0.5 equivalent of 2a was used, NR-No reaction.

At first, the reaction was carried out at 50 °C in CH_3CN by taking 1 equivalent of each of the substrates. To our delight, within 2 hours the reaction mixture appeared in light pink and the solution precipitated. Complete consumption of starting materials (vide TLC) was observed with the formation of the C3 benzylated product (100% yield) (entry **1**, Table **4.1**). Inspired by this result, we carried out the reaction at room temperature keeping the other parameters constant, and the reaction proceeded smoothly by consuming the substrates completely (entry **2**, Table **4.1**). In alcoholic medium (EtOH, *i*PrOH, MeOH), the reaction afforded low yields of the desired product (entries **3**-**5**, Table **4.1**). In toluene also, there was no significant improvement in the yield (entry **6**, Table **4.1**). On the other hand, the reaction failed in aqueous and other polar solvents (entries **7**, **8**-**10**, Table **4.1**). By reducing the amount of trityl chloride to 0.5 equivalent, 54% yield of the C-3 benzylated product was obtained (entry **11**, Table **4.1**). The efficiency of this C-3 benzylation depends on the nature of the solvent utilized in the reaction. CH_3CN acts as Lewis base [15b] and lone pair of electrons on the nitrogen atom may easily polarize the chlorine atom of trityl chloride by inducing a positive potential [20]. This induced positive potential may create the σ-hole and hence complex formation takes place between CH_3CN and trityl chloride through halogen bonding.

4.3.2 Substrate scope study

After optimization, we further studied the scope and limitations of electronically and sterically diverse substrates and the results are shown in Table **4.2**.

Table **4.2**. C-3 benzylation of indoles with trityl chloride derivatives[a]

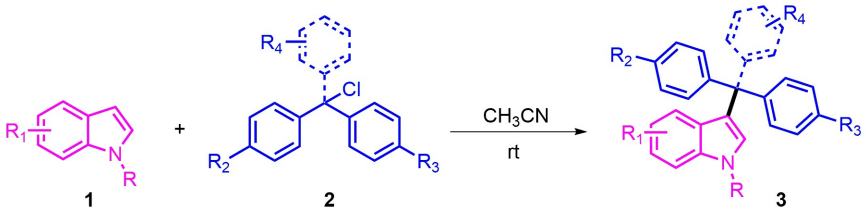

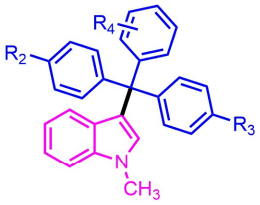

3aa, R_2, R_3, R_4 = H, 100%
3ab, R_2, R_3 = OCH_3, R_4 = H, 90%
3ac, R_2, R_3 = H, R_4 = 4-CH_3, 100%
3ad, R_2, R_3 = H, R_4 = 2-Cl, 82%
3ae, R_2, R_3 = H, R_4 = 4-OCH_3, 88%

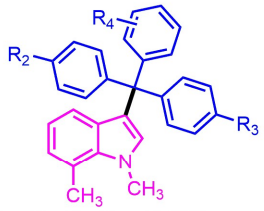

3ba, R_2, R_3, R_4 = H, 98%
3bb, R_2, R_3 = OCH_3, R_4 = H, 87%
3bc, R_2, R_3 = H, R_4 = 4-CH_3, 76%
3bd, R_2, R_3 = H, R_4 = 4-OCH_3, 74%

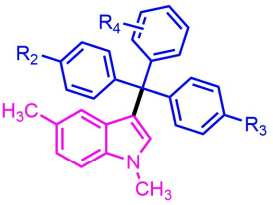

3ca, R_2, R_3, R_4 = H, 99%
3cb, R_2, R_3 = OCH_3, R_4 = H, 87%
3cc, R_2, R_3 = H, R_4 = 4-CH_3, 77%
3cd, R_2, R_3 = H, R_4 = 4-OCH_3, 71%

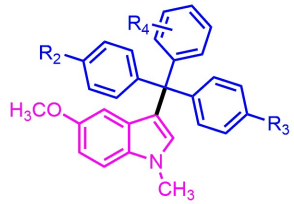

3da, R_2, R_3, R_4 = H, 99%
3db, R_2, R_3 = OCH_3, R_4 = H, 87%

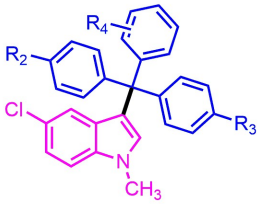

3ea, R_2, R_3, R_4 = H, 95%
3eb, R_2, R_3 = OCH_3, R_4 = H, 84%[b]
3ec, R_2, R_3 = H, R_4 = 4-CH_3, 87%

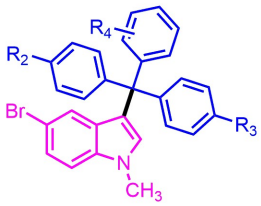

3fa, R_2, R_3, R_4 = H, 36%
3fb, R_2, R_3 = OCH_3, R_4 = H, 63%

3ga, R_2, R_3, R_4 = H, 98%[c]
3gb, R_2, R_3 = OCH_3, R_4 = H, 89%[c]
3gc, R_2, R_3 = H, R_4 = 4-CH_3, 85%[c]
3gd, R_2, R_3 = H, R_4 = 4-OCH_3, 91%[c]

3h, 62%[d]

3i, 58%

[a]Reaction conditions: **1** (1 equiv.), **2** (1 equiv.), CH_3CN (2 mL), 2 hours, [b]3 hours, [c]8 hours, [d]5 hours.

Differently substituted indole and trityl chloride derivatives reacted smoothly, furnishing the C-3 substituted product in moderate to excellent yields (36-100%). Both *N*-methyl and *N*-H indoles were compatible with the optimized reaction conditions. *N*-methylindoles having electron-donating (-OCH_3,-CH_3) (**3ba-3bd**, **3ca-3cd**, **3da**, **3db**, Table **4.2**) and withdrawing-groups (-Cl, -Br) (**3ea-3ec**, **3fa**, **3fb**, Table **4.2**) proceeded the reaction efficiently. Similarly, electron-rich (-OCH_3, -CH_3) (**3ab**, **3ae**, **3bb-3bd**, **3cb-3cd**, **3db**, **3eb**, **3ec**, **3fb**, **3gb-3gd**, Table **4.2**) and deficient (-Cl) (**3ad**, Table **4.2**) trityl chlorides were also well-tolerable to the current protocol. The reaction afforded column chromatography-free isolation of products for some of the substrates (**3aa**, **3ac**, **3ba**, **3ca**,

3da, **3ga**, Table **4.2**) with excellent yields (98-100%). *N*-methylindole having $–CH_3$ group at the C-2 position (**3h**, Table **4.2**) resulted in a moderate yield (62%) of the desired product which might be due to the steric effect. The reaction failed in the case of C-3-protected *N*-methylindole indicating that the benzylation is only feasible at the C-3 position. Similar to *N*-methylindoles, in our protocol, the benzylation of *N*-H indole occurs at the C-3 position without affecting the N1 position due to the high nucleophilicity of C-3 rather than N1. Like trityl chloride, chlorodiphenylmethane is also an active benzylating agent under the optimized conditions and afforded 58% yield of the targeted product (**3i**, Table **4.2**).

To further extend the applicability of this methodology, we have tried to benzylate other nitrogen-containing heterocycles including pyrrole, imidazole, and piperidine derivatives. But the developed methodology is not suitable for the *N*-benzylation of pyrrole and piperidine derivatives. For the *N*-benzylation of imidazole, the current protocol is not effective in 2 hours at room temperature. Then we increased the reaction time to 24 hours, but we could not get a satisfactory result. Increasing the temperature up to 60 °C (for 24 hours) was also ineffective to furnish the *N*-benzylated product. Following these experiments, we again repeated the reaction at room temperature and the formation of the desired product was observed after 48 hours. The effectiveness of various substituents in the *N*-benzylation of imidazoles was studied and the results are shown in Table **4.3**. Electron-donating or withdrawing groups present in imidazole and trityl chloride reacted efficiently with low to good yields (20-81%) of *N*-benzylated products. Chlorodiphenylmethane was also utilized for the *N*-benzylation of imidazole and resulted in a comparatively low yield (28%) (**4h**, Table **4.3**). In imidazoles, the nitrogen atom attached to hydrogen acts as a better nucleophile since this hydrogen is more acidic as compared to the hydrogen atom attached to carbon and hence benzylation occurs at the N-H position rather than the carbon atom [21].

With this catalyst-free methodology, the synthesis of a pharmaceutically active compound, **Clotrimazole** (antimycotic agent) was done and we were able to isolate the product up to 67% yield (**4i**, Table **4.3**).

Table **4.3**. Substrate scope for the reaction between imidazole and trityl chloride derivatives:[a]

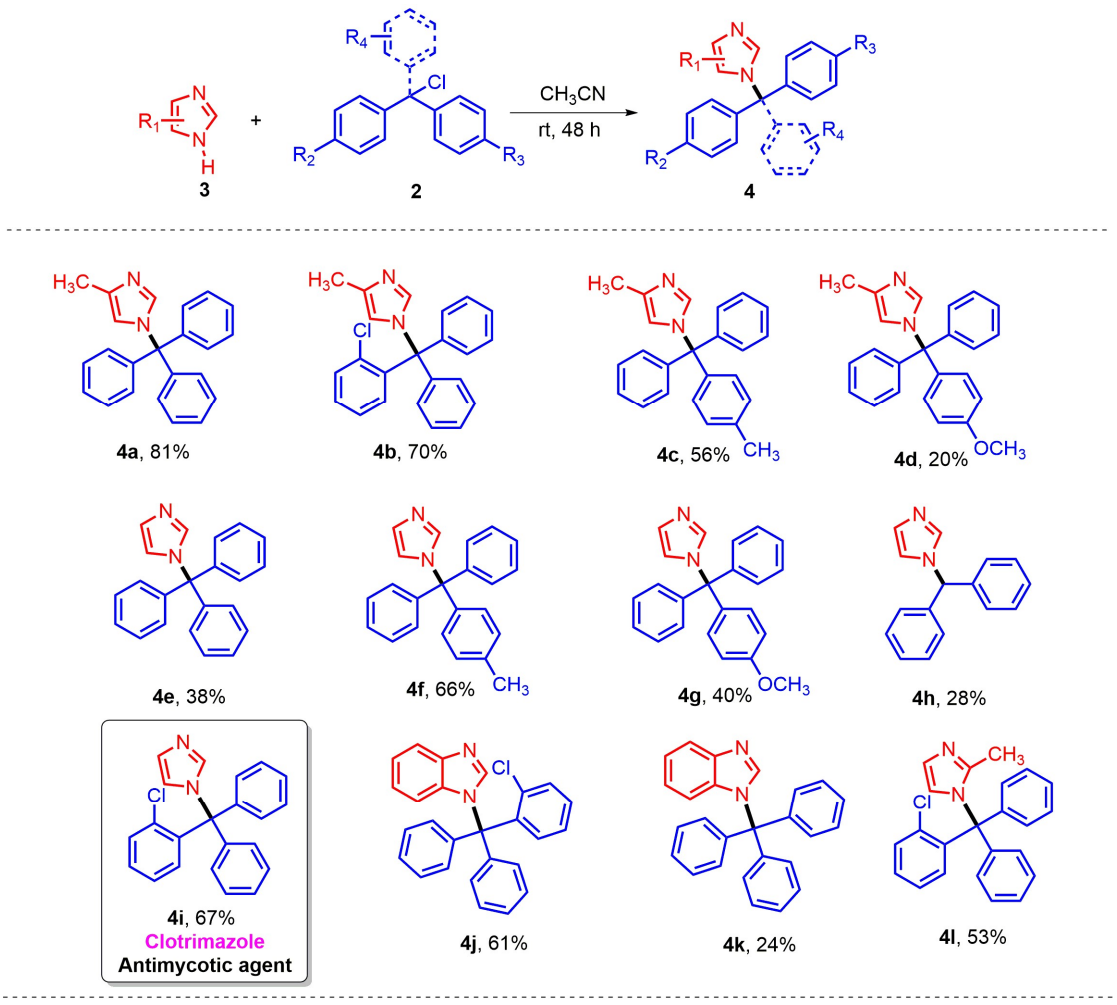

[a]Reaction conditions: **3** (1 equiv.), **2** (1 equiv.), CH_3CN (2mL).

4.3.3 Mechanism study

To study the halogen bonding formation, the reaction mixture of only trityl chloride in CH_3CN (after 2 hours of stirring at room temperature) was used for UV-Vis and FT-IR (Figure **4.3**) analyses. In the UV spectra (Figure **4.3a**), the maximum absorption for trityl chloride appeared at 240 nm. Conversely, the complex of trityl chloride and CH_3CN showed a maximum absorption peak at 204 nm. This blue shifting (36 nm) of wavelength interpreted the formation of trityl chloride-CH_3CN complex *via* halogen bonding [22]. Since in our methodology, the reaction was not feasible in DMF so, we carried out the UV-Vis analysis of trityl chloride and DMF mixture and the maximum absorption peak appeared at 227 nm. But the shifting of wavelength (13 nm) was low in

DMF, which might indicate the weak or less favourable or somewhat repulsive interaction with trityl chloride (if deviated from the σ-hole region) due to the planar structure of DMF.

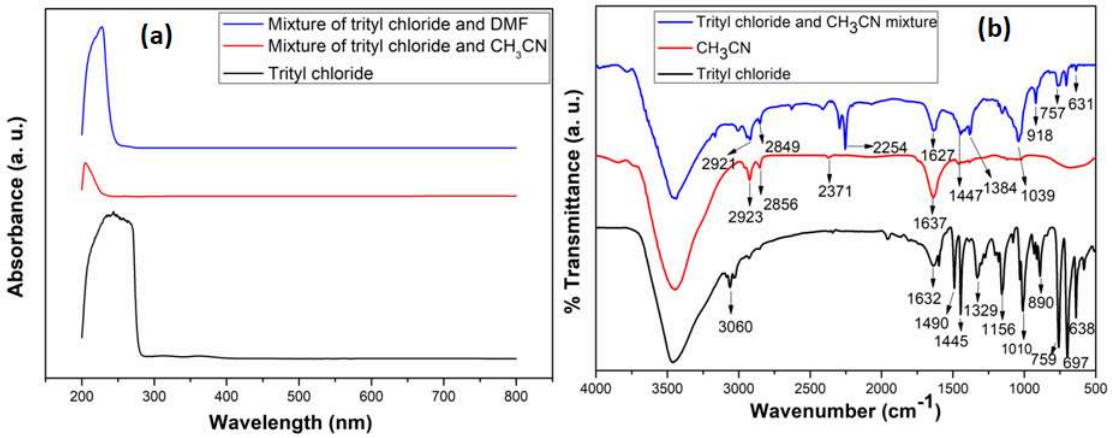

Figure **4.3**. (**a**) UV-Vis spectra of trityl chloride and mixtures in CH_3CN and DMF at room temperature in ethanol; (**b**) FT-IR spectra trityl chloride, CH_3CN, and mixture of CH_3CN and trityl chloride

The peak appears at 638 cm^{-1} in the FT-IR spectrum (Figure **4.3b**) of trityl chloride is due to C-Cl bond stretching. Similarly, alkyl C-H stretching of CH_3CN appears at 2923 and 2856 cm^{-1}. The peak at 2371 cm^{-1} is due to the C≡N bond stretching of CH_3CN. But the FT-IR spectrum of trityl chloride and CH_3CN mixture shows that alkyl C-H (2921, 2849 cm^{-1}), C≡N (2254 cm^{-1}) and C-Cl (631 cm^{-1}) bond stretching frequencies are shifted to lower wavenumber, indicating the decrease of bond strength which may be due to the complex formation between them through halogen bonding [16,22,23]. From UV-Vis and FT-IR analyses it is seen that CH_3CN plays the key role to carry out the benzylation through halogen bonding.

4.3.4 Plausible mechanism

Based on the spectroscopic studies, a possible mechanism for halogen bond formation in CH_3CN was proposed (Scheme **4.2**). Trityl chloride has not a positive potential on the chlorine atom due to the higher electronegativity as compared to the carbon [16,20,24]. The Lewis basic nature of CH_3CN polarized the chlorine atom by inducing a positive potential which we might consider as the σ-hole, and then facilitated the formation of complex **A**. Complex **A** then generated intermediate **B**, which finally furnished the desired product. The linear structure of CH_3CN might be favourable in retaining the

proper directionality of the halogen bonding interaction by limiting the deviation from the σ-hole.

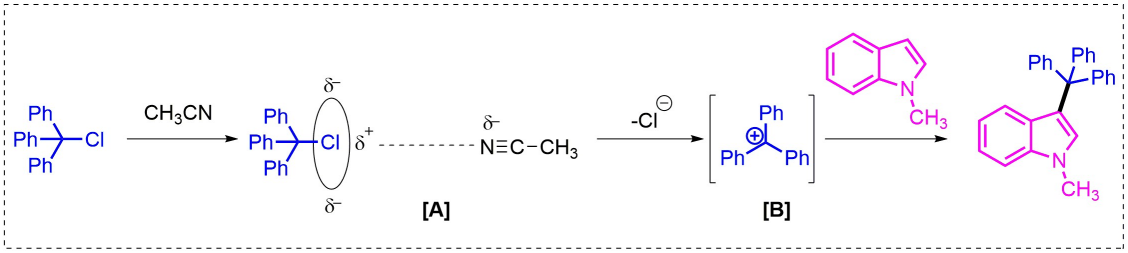

Scheme **4.2**. Possible mechanism for C-3 benzylation of indole through halogen bonding

4.4 Conclusion

In summary, we have developed a new protocol for CH_3CN mediated C-3 and *N*-benzylation of nitrogen-rich heterocycles using trityl chlorides through halogen bonding at room temperature under catalyst-free conditions. Both protected and unprotected indole derivatives proceed the reaction with equal efficiency under the developed reaction conditions. In absence of an external base, trityl chlorides can easily benzylate imidazole derivatives at the nitrogen atom. This transition metal-free methodology is applicable for a broad range of substrates with moderate to excellent yields of the targeted products. The mechanistic pathway indicates the existence of halogen bonding which is further proved by UV-Vis and FT-IR analyses. The cleavage of the C-Cl bond is offered by CH_3CN because of its Lewis basic nature that enhances the halogen bonding. This simple and easy protocol is environmentally benign, affording the desired product under catalyst-, base-, and ligand-free conditions.

4.5 ^{1}H and ^{13}C NMR analytical data

3aa

1-methyl-3-trityl-1*H*-indole (3aa): ^{1}H NMR (400 MHz, $CDCl_3$): δ (ppm) 7.31–7.08 (m, 18H), 6.77 (t, J = 7.5 Hz, 1H), 6.65 (d, J = 8.8 Hz, 2H), 3.70 (s, 3H); ^{13}C NMR (100 MHz, $CDCl_3$): δ (ppm) 146.7, 137.7, 130.8, 130.2, 128.3, 128.0, 127.4, 126.0, 122.9, 122.3, 121.3, 118.7, 109.0, 59.5, 32.8.

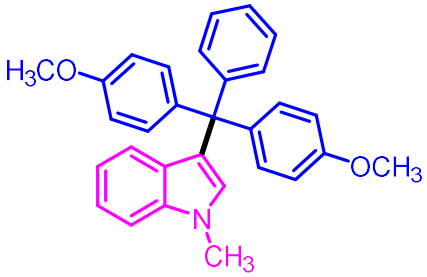

3ab

3-(bis(4-methoxyphenyl)(phenyl)methyl)-1-methyl-1*H*-indole (3ab): ^{1}H NMR (400 MHz, $CDCl_3$): δ (ppm) 7.32–7.13 (m, 12H), 6.86–6.76 (m, 5H), 6.72–6.65 (m, 2H), 3.81 (s, 6H), 3.74 (s, 3H); ^{13}C NMR (100 MHz, $CDCl_3$): δ (ppm) 157.5, 147.2, 139.2, 137.7, 131.7, 130.6, 130.0, 128.3, 127.3, 125.9, 123.0, 122.8, 121.2, 118.7, 112.6, 109.0, 58.0, 55.2, 32.7.

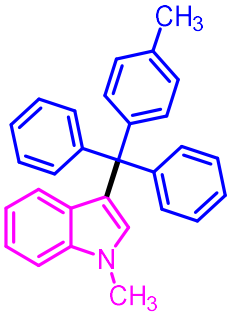

3ac

3-(diphenyl(*p*-tolyl)methyl)-1-methyl-1*H*-indole (3ac): ^{1}H NMR (400 MHz, $CDCl_3$): δ (ppm) 7.22–7.00 (m, 15H), 6.95 (d, J = 7.5 Hz, 2H), 6.70 (t, J = 7.5 Hz, 1H), 6.61–6.56 (m, 2H), 3.62 (s, 3H), 2.23 (s, 3H); ^{13}C NMR (100 MHz, $CDCl_3$): δ (ppm) 146.8, 143.7, 137.7, 135.4, 130.8, 130.7, 130.2, 128.3, 128.1, 127.4, 125.9, 123.0, 122.4, 121.2, 118.6, 109.0, 59.1, 32.8, 21.0.

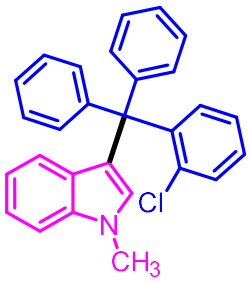

3ad

3-((2-chlorophenyl)diphenylmethyl)-1-methyl-1*H*-indole (3ad): ^{1}H NMR (400 MHz, $CDCl_3$): δ (ppm) 7.43–7.11 (m, 17H), 6.79 (t, J = 7.6 Hz, 1H), 6.69–6.57 (m, 2H), 3.74 (s, 3H); ^{13}C NMR (100 MHz, $CDCl_3$): δ (ppm) 144.3, 144.0, 137.6, 136.4, 132.4, 131.9, 130.8, 128.2, 128.1, 127.3, 126.2, 126.0, 122.2, 121.2, 121.0, 118.8, 109.0, 59.8, 32.8.

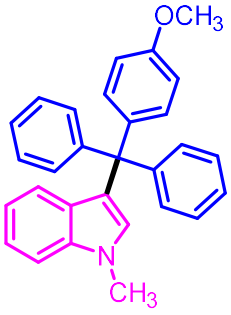

3ae

3-((4-methoxyphenyl)diphenylmethyl)-1-methyl-1*H*-indole (3ae): ^{1}H NMR (400 MHz, $CDCl_3$): δ (ppm) 7.32–7.22 (m, 12H), 7.20–7.14 (m, 3H), 6.85–6.79 (m, 3H), 6.71 (d, J = 9.7 Hz, 2H), 3.82 (s, 3H), 3.75 (s, 3H); ^{13}C NMR (100 MHz, $CDCl_3$): δ (ppm) 157.6, 146.9, 138.9, 137.7, 131.8, 130.7, 130.1, 128.3, 127.4, 125.9, 123.0, 122.5, 121.2, 118.7,

112.6, 109.0, 58.7, 55.2, 32.8.

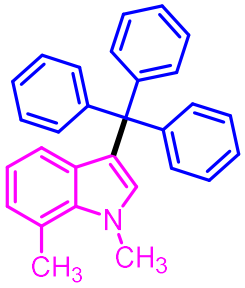

3ba

1,7-dimethyl-3-trityl-1*H*-indole (3ba): ^{1}H NMR (400 MHz, $CDCl_3$): δ (ppm) 7.31–7.27 (m, 5H), 7.21 (s, 11H), 6.79 (d, J = 6.9 Hz, 1H), 6.61 (t, J = 7.6 Hz, 1H), 6.55–6.47 (m, 2H), 3.96 (s, 3H), 2.74 (s, 3H); ^{13}C NMR (100 MHz, $CDCl_3$): δ (ppm) 146.6, 132.1, 130.8, 129.3, 128.0, 127.3, 125.9, 124.0, 121.8, 121.2, 120.8, 118.8, 59.4, 36.9, 19.9.

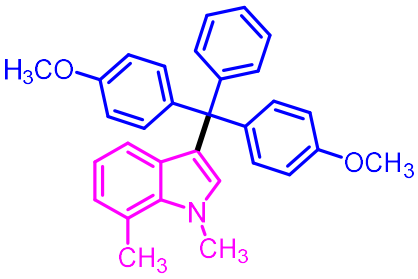

3bb

3-(bis(4-methoxyphenyl)(phenyl)methyl)-1,7-dimethyl-1*H*-indole (3bb): ^{1}H NMR (400 MHz, $CDCl_3$): δ (ppm) 7.14–7.09 (m, 5H), 7.08–7.00 (m, 4H), 6.73–6.65 (m, 5H), 6.58–6.53 (m, 1H), 6.43 (d, J = 8.7 Hz, 2H), 3.88 (d, J = 4.6 Hz, 3H), 3.69 (s, 6H), 2.67 (s, 3H); ^{13}C NMR (100 MHz, $CDCl_3$): δ (ppm) 157.5, 147.1, 139.1, 136.5, 131.9, 131.7, 130.6, 129.3, 127.3, 125.8, 123.9, 122.3, 121.3, 120.8, 118.8, 112.6, 58.0, 55.2, 36.9, 19.9.

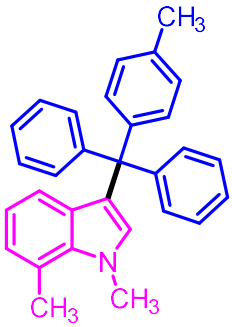

3bc

3-(diphenyl(*p*-tolyl)methyl)-1,7-dimethyl-1*H*-indole (3bc): ^{1}H NMR (400 MHz, $CDCl_3$): δ (ppm) 7.17–7.08 (m, 10H), 7.01 (d, J = 8.3 Hz, 2H), 6.94 (d, J = 8.2 Hz, 2H), 6.71 (d, J = 7.0 Hz, 1H), 6.57–6.51 (m, 1H), 6.47–6.40 (m, 2H), 3.88 (s, 3H), 2.67 (s, 3H), 2.23 (s, 3H); ^{13}C NMR (100 MHz, $CDCl_3$): δ (ppm) 146.7, 143.6, 136.5, 135.4, 132.0, 130.8, 130.7, 129.3, 128.1, 127.3, 125.9, 124.0, 121.9, 121.3, 120.8, 118.8, 59.0, 36.9, 21.0, 19.9.

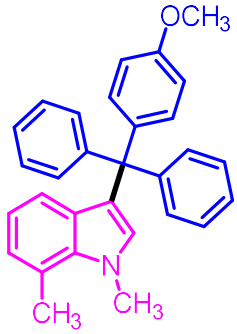

3bd

3-((4-methoxyphenyl)diphenylmethyl)-1,7-dimethyl-1*H*-indole (3bd): ^{1}H NMR (400 MHz, $CDCl_3$): δ (ppm) 7.17–7.07 (m, 10H), 7.06–7.01 (m, 2H), 6.75–6.64 (m, 3H), 6.58–6.51 (m, 1H), 6.42 (d, J = 8.9 Hz, 2H), 3.88 (s, 3H), 3.70 (d, J = 7.8 Hz, 3H), 2.67 (s, 3H); ^{13}C NMR (100 MHz, $CDCl_3$): δ (ppm) 157.6, 146.9, 138.8, 136.5, 132.0, 131.8, 130.7, 129.3, 127.3, 125.9, 124.0, 122.0, 121.3, 120.8, 118.8, 112.6, 58.7, 55.2, 36.9, 19.9.

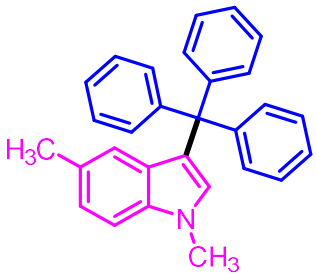

3ca

1,5-dimethyl-3-trityl-1*H*-indole (3ca): ^{1}H NMR (400 MHz, $CDCl_3$): δ (ppm) 7.32–7.26 (m, 5H), 7.21 (dd, J = 7.4, 2.6 Hz, 10H), 7.14 (d, J = 8.3 Hz, 1H), 6.97–6.92 (m, 1H), 6.60 (s, 1H), 6.40 (s, 1H), 3.67 (s, 3H), 2.14 (s, 3H); ^{13}C NMR (100 MHz, $CDCl_3$): δ (ppm) 146.6, 136.2, 130.8, 130.4, 128.6, 127.9, 127.3, 125.9, 122.9, 122.5, 121.6, 108.6, 59.4, 32.8, 21.5.

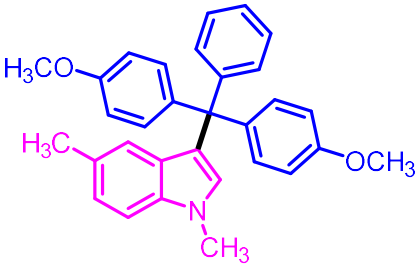

3cb

3-(bis(4-methoxyphenyl)(phenyl)methyl)-1,5-dimethyl-1*H*-indole (3cb): ^{1}H NMR (400 MHz, $CDCl_3$): δ (ppm) 7.29–7.22 (m, 5H), 7.17 (t, J = 8.1 Hz, 5H), 6.99 (t, J = 8.3 Hz, 1H), 6.80 (d, J = 8.9 Hz, 4H), 6.61 (s, 1H), 6.48 (s, 1H), 3.82 (s, 6H), 3.71 (s, 3H), 2.20 (s, 3H); ^{13}C NMR (100 MHz, $CDCl_3$): δ (ppm) 157.5, 147.3, 139.2, 136.2, 131.7, 130.7, 130.2, 128.5, 127.6, 127.3, 125.8, 122.9, 122.6, 122.2, 112.6, 108.6, 58.0, 55.2, 32.8, 21.5.

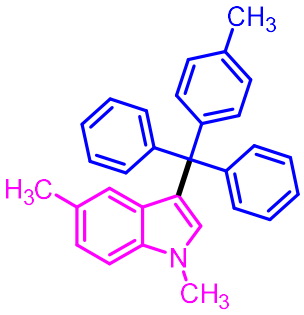

3cc

3-(diphenyl(*p*-tolyl)methyl)-1,5-dimethyl-1*H*-indole (3cc): ^{1}H NMR (400 MHz, $CDCl_3$): δ (ppm) 7.17–7.00 (m, 13H), 6.95 (d, J = 8.3 Hz, 2H), 6.88–6.84 (m, 1H), 6.52 (s, 1H), 6.34 (s, 1H), 3.59 (s, 3H), 2.24 (s, 3H), 2.07 (s, 3H); ^{13}C NMR (100 MHz, $CDCl_3$): δ (ppm) 146.8, 143.8, 136.2, 135.3, 130.8, 130.7, 130.3, 128.5, 128.1, 127.6, 127.3, 125.8, 122.9, 122.6, 121.8, 108.6, 59.1, 32.8, 21.5, 21.0.

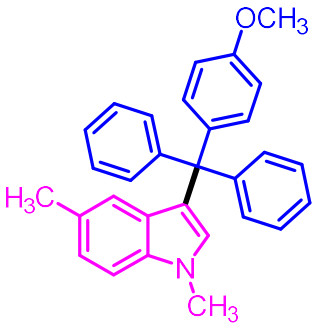

3cd

3-((4-methoxyphenyl)diphenylmethyl)-1,5-dimethyl-1*H*-indole (3cd): ^{1}H NMR (400 MHz, $CDCl_3$): δ (ppm) 7.29–7.13 (m, 14H), 6.97 (d, J = 8.3 Hz, 1H), 6.80 (t, J = 6.0 Hz, 2H), 6.62 (s, 1H), 6.45 (s, 1H), 3.81 (s, 3H), 3.71 (s, 3H), 2.18 (s, 3H); ^{13}C NMR (100 MHz, $CDCl_3$): δ (ppm) 157.5, 147.0, 138.9, 136.2, 131.8, 130.7, 130.2, 128.5, 127.6, 127.3, 125.8, 122.9, 122.6, 121.9, 112.6, 108.6, 58.7, 55.2, 32.8, 21.5.

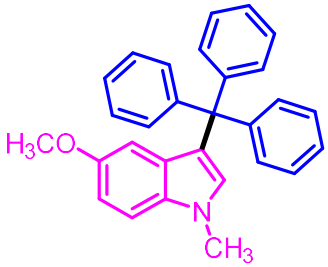

3da

5-methoxy-1-methyl-3-trityl-1*H*-indole (3da): ^{1}H NMR (400 MHz, $CDCl_3$): δ (ppm) 7.31–7.27 (m, 2H), 7.24–7.18 (m, 14H), 7.12 (d, J = 8.8 Hz, 1H), 6.76 (dd, J = 8.8, 2.5 Hz, 1H), 6.64 (s, 1H), 6.03 (d, J = 2.4 Hz, 1H), 3.67 (s, 3H), 3.37 (s, 3H); ^{13}C NMR (100 MHz, $CDCl_3$): δ (ppm) 153.1, 146.6, 133.1, 130.8, 128.6, 127.9, 127.4, 125.9, 121.7, 111.6, 109.5, 104.4, 59.4, 55.5, 32.9.

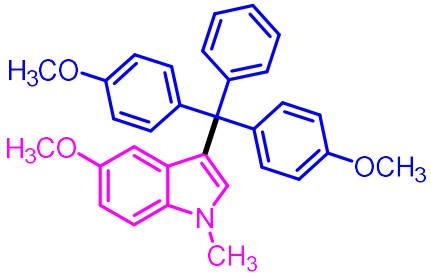

3db

3-(bis(4-methoxyphenyl)(phenyl)methyl)-5-methoxy-1-methyl-1*H*-indole (3db): ^{1}H NMR (400 MHz, $CDCl_3$): δ (ppm) 7.31–7.15 (m, 10H), 6.83 (t, J = 5.8 Hz, 5H), 6.68 (s, 1H), 6.13 (d, J = 1.8 Hz, 1H), 3.82 (s, 6H), 3.71 (s, 3H), 3.46 (s, 3H); ^{13}C NMR (100 MHz, $CDCl_3$): δ (ppm) 157.6, 153.0, 147.2, 139.2, 133.1, 131.7, 130.7, 130.5, 128.6, 127.4, 125.9, 122.4, 112.6, 111.6, 109.7, 104.5, 58.0, 55.2, 32.9.

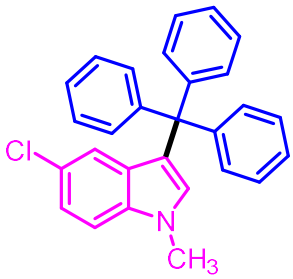

3ea

5-chloro-1-methyl-3-trityl-1*H*-indole (3ea): ^{1}H NMR (400 MHz, $CDCl_3$): δ (ppm) 7.34–7.16 (m, 16H), 7.09 (dd, J = 8.7, 2.0 Hz, 1H), 6.74 (s, 1H), 6.62 (d, J = 1.9 Hz, 1H), 3.72 (s, 3H); ^{13}C NMR (100 MHz, $CDCl_3$): δ (ppm) 146.2, 136.1, 131.3, 130.7, 129.2, 128.0, 127.5, 126.2, 124.5, 122.0, 121.7, 110.1, 59.3, 33.0.

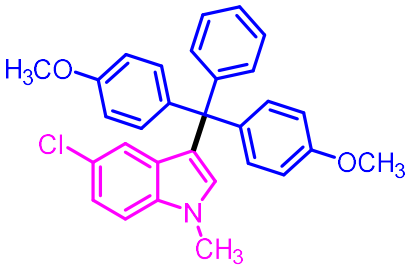

3eb

3-(bis(4-methoxyphenyl)(phenyl)methyl)-5-chloro-1-methyl-1*H*-indole (3eb): ^{1}H NMR (400 MHz, $CDCl_3$): δ (ppm) 7.17–6.95 (m, 12H), 6.68 (d, J = 8.9 Hz, 4H), 6.59–6.53 (m, 2H), 3.70 (s, 6H), 3.59 (s, 3H); ^{13}C NMR (100 MHz, $CDCl_3$): δ (ppm) 157.7, 146.8, 138.7, 136.1, 131.6, 131.2, 130.5, 129.2, 127.5, 126.0, 124.5, 122.6, 122.0, 121.7, 112.7, 110.1, 57.9, 55.2, 32.9.

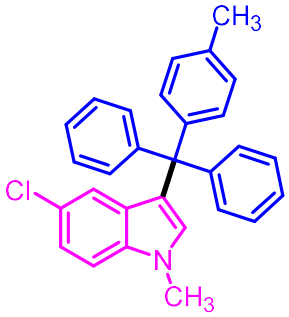

3ec

5-chloro-3-(diphenyl(*p*-tolyl)methyl)-1-methyl-1*H*-indole (3ec): ^{1}H NMR (400 MHz, $CDCl_3$): δ (ppm) 7.19–6.94 (m, 16H), 6.62 (s, 1H), 6.52 (s, 1H), 3.61 (s, 3H), 2.25 (s, 3H); ^{13}C NMR (100 MHz, $CDCl_3$): δ (ppm) 146.4, 143.3, 136.1, 135.6, 131.3, 130.7, 130.5, 129.2, 128.2, 127.5, 126.1, 124.5, 122.2, 122.0, 121.7, 110.1, 58.9, 32.9, 21.0.

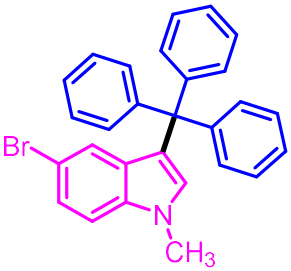

3fa

5-bromo-1-methyl-3-trityl-1*H*-indole (3fa): ^{1}H NMR (400 MHz, $CDCl_3$): δ (ppm) 7.19–7.10 (m, 16H), 7.04 (d, J = 8.7 Hz, 1H), 6.64 (d, J = 1.8 Hz, 1H), 6.60 (d, J = 3.6 Hz, 1H), 3.61 (s, 3H); ^{13}C NMR (100 MHz, $CDCl_3$): δ (ppm) 146.2, 136.4, 131.2, 130.7, 129.8, 127.5, 126.1, 125.0, 124.3, 122.0, 112.2, 110.6, 59.3, 32.9.

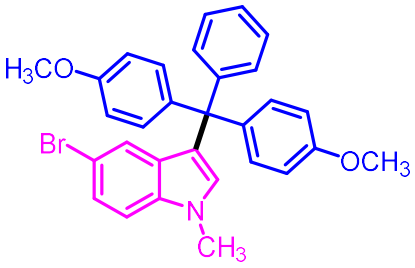

3fb

3-(bis(4-methoxyphenyl)(phenyl)methyl)-5-bromo-1-methyl-1*H*-indole (3fb): ^{1}H NMR (400 MHz, $CDCl_3$): δ (ppm) 7.30–7.10 (m, 12H), 6.85–6.77 (m, 5H), 6.68 (s, 1H), 3.82 (s, 6H), 3.71 (s, 3H); ^{13}C NMR (100 MHz, $CDCl_3$): δ (ppm) 157.7, 146.8, 138.7, 136.4, 131.6, 131.0, 130.5, 129.8, 127.5, 126.0, 125.1, 124.2, 122.6, 112.7, 112.2, 110.6, 57.9, 55.2, 32.9.

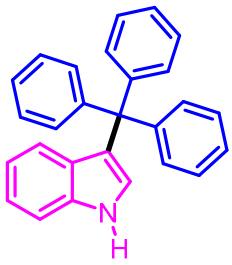

3ga

3-trityl-1*H*-indole (3ga): ^{1}H NMR (400 MHz, $CDCl_3$): δ (ppm) 7.90 (s, 1H), 7.33–7.16 (m, 17H), 7.08 (t, J = 7.6 Hz, 1H), 6.78 (dd, J = 11.0, 4.3 Hz, 2H), 6.67 (d, J = 8.1 Hz, 1H); ^{13}C NMR (100 MHz, $CDCl_3$): δ (ppm) 146.5, 137.0, 130.8, 128.0, 127.8, 127.4, 126.0, 125.5, 124.0, 122.8, 121.7, 119.2, 111.0, 59.5.

3gb

3-(bis(4-methoxyphenyl)(phenyl)methyl)-1*H*-indole (3gb): ^{1}H NMR (400 MHz, $CDCl_3$): δ (ppm) 7.96 (s, 1H), 7.36–7.10 (m, 13H), 6.88–6.71 (m, 8H), 3.81 (s, 6H); ^{13}C NMR (100 MHz, $CDCl_3$): δ (ppm) 157.6, 147.1, 139.0, 137.0, 131.7, 130.6, 127.8, 127.4, 125.9, 125.3, 124.5, 122.9, 121.7, 119.2, 112.6, 110.9, 58.0, 55.2.

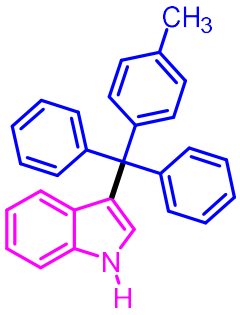

3gc

3-(diphenyl(*p*-tolyl)methyl)-1*H*-indole (3gc): ^{1}H NMR (400 MHz, $CDCl_3$): δ (ppm) 7.68 (s, 1H), 7.20–6.95 (m, 19H), 6.91 (d, J = 8.1 Hz, 2H), 6.67 (m, 2H), 6.59 (d, J = 8.1 Hz, 1H), 2.20 (s, 3H); ^{13}C NMR (100 MHz, $CDCl_3$): δ (ppm) 146.7, 143.5, 137.0, 135.5, 130.8, 130.7, 128.7, 128.1, 127.9, 127.4, 127.2, 126.0, 125.5, 124.1, 122.9, 121.7, 119.2, 110.9, 59.1, 21.0.

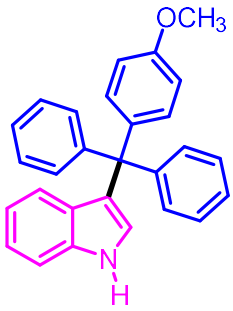

3gd

3-((4-methoxyphenyl)diphenylmethyl)-1*H*-indole (3gd): ^{1}H NMR (400 MHz, $CDCl_3$): δ (ppm) 7.83 (s, 1H), 7.25–7.18 (m, 2H), 7.17–7.07 (m, 10H), 7.06–6.98 (m, 3H), 6.77–6.58 (m, 5H), 3.68 (d, J = 4.3 Hz, 3H); ^{13}C NMR (100 MHz, $CDCl_3$): δ (ppm) 157.6, 146.8, 138.7, 137.0, 131.8, 137.0, 131.8, 130.7, 127.9, 127.8, 127.4, 126.0, 125.4, 124.2, 122.9, 121.7, 119.2, 112.6, 111.0, 58.7, 55.2.

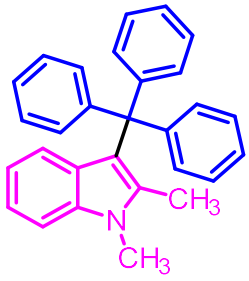

3h

1,2-dimethyl-3-trityl-1*H*-indole (3h): ^{1}H NMR (400 MHz, $CDCl_3$): δ (ppm) 7.43 (m, 6H), 7.24–7.11 (m, 10H), 7.03 (m, 1H), 6.73 (m, 1H), 6.40 (d, J = 8.2 Hz, 1H), 3.60 (s, 3H), 1.82 (s, 3H); ^{13}C NMR (100 MHz, $CDCl_3$): δ (ppm) 147.1, 136.8, 134.9, 130.6, 127.4, 125.5, 122.0, 120.0, 118.3, 117.7, 108.3, 60.3, 29.5, 13.8.

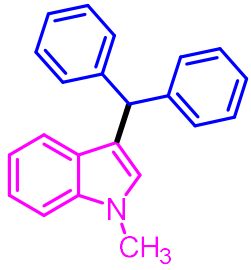

3i

3-benzhydryl-1-methyl-1*H*-indole (3i): ^{1}H NMR (400 MHz, $CDCl_3$): δ (ppm) 7.21–7.05 (m, 15H), 6.90–6.83 (m, 1H), 6.30 (s, 1H), 5.57 (s, 1H), 3.53 (s, 3H); ^{13}C NMR (100 MHz, $CDCl_3$): δ (ppm) 144.2, 142.3, 137.6, 129.1, 128.8, 128.5, 128.4, 127.6, 127.5, 127.4, 126.3, 121.7, 120.1, 118.9, 118.4, 109.2, 48.9, 32.7.

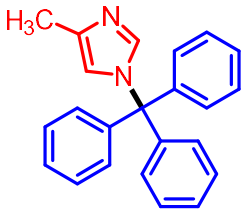

4a

4-methyl-1-trityl-1*H*-imidazole (4a): ^{1}H NMR (400 MHz, $CDCl_3$): δ (ppm) 7.38–7.32 (m, 10H), 7.17 (dd, J = 6.2, 3.5 Hz, 6H), 6.54 (s, 1H), 2.22 (s, 3H); ^{13}C NMR (100 MHz, $CDCl_3$): δ (ppm) 142.6, 138.2, 137.1, 129.8, 128.0, 127.9, 118.2, 75.0, 13.9.

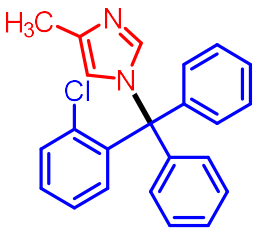

4b

1-((2-chlorophenyl)diphenylmethyl)-4-methyl-1*H*-imidazole (4b): ^{1}H NMR (400 MHz, $CDCl_3$): δ (ppm) 7.32–7.19 (m, 9H), 7.18–7.07 (m, 5H), 6.85 (dd, J = 8.0, 1.6 Hz, 1H), 6.34 (s, 1H), 2.09 (s, 3H); ^{13}C NMR (100 MHz, $CDCl_3$): δ (ppm) 141.0, 140.3, 138.2, 137.0, 135.5, 132.2, 130.4, 130.2, 129.8, 128.1, 128.0, 127.0, 118.0, 75.0, 13.7.

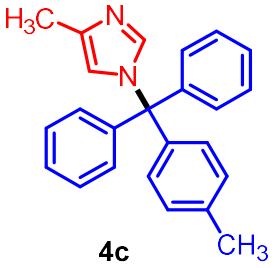

4c

1-(diphenyl(*p*-tolyl)methyl)-4-methyl-1*H*-imidazole (4c): ^{1}H NMR (400 MHz, $CDCl_3$): δ (ppm) 7.39–7.27 (m, 7H), 7.16 (m, 6H), 7.04 (d, J = 8.3 Hz, 2H), 6.54 (s, 1H), 2.38 (s, 3H), 2.22 (s, 3H); ^{13}C NMR (100 MHz, $CDCl_3$): δ (ppm) 142.8, 139.7, 138.2, 137.7, 137.1, 129.8, 128.7, 127.9, 118.1, 74.8, 21.0, 13.9.

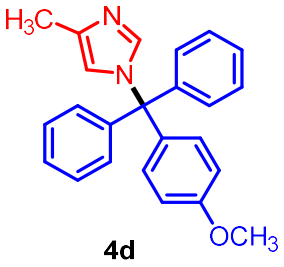

4d

1-((4-methoxyphenyl)diphenylmethyl)-4-methyl-1*H*-imidazole (4d): ^{1}H NMR (400 MHz, $CDCl_3$): δ (ppm) 7.37–7.30 (m, 7H), 7.18–7.12 (m, 4H), 7.09–7.05 (m, 2H), 6.88–6.83 (m, 2H), 6.53 (s, 1H), 3.83 (s, 3H), 2.22 (s, 3H); ^{13}C NMR (100 MHz, $CDCl_3$): δ (ppm) 159.0, 142.9, 138.1, 137.0, 134.7, 131.2, 129.7, 127.9, 118.1, 113.2, 74.6, 55.3, 13.9.

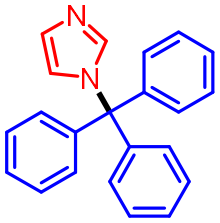

4e

1-trityl-1*H*-imidazole (4e): ^{1}H NMR (400 MHz, $CDCl_3$): δ (ppm) 7.39 (s, 1H), 7.29–7.21 (m, 9H), 7.10–7.02 (m, 6H), 6.99 (s, 1H), 6.75 (s, 1H); ^{13}C NMR (100 MHz, $CDCl_3$): δ (ppm) 142.5, 139.0, 129.8, 128.3, 128.1, 121.7, 75.2.

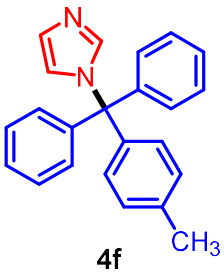

4f

1-(diphenyl(*p*-tolyl)methyl)-1*H*-imidazole (4f): ^{1}H NMR (400 MHz, $CDCl_3$): δ (ppm) 7.49 (s, 1H), 7.39–7.28 (m, 6H), 7.16 (m, 6H), 7.10–7.02 (m, 3H), 6.85 (s, 1H), 2.38 (s, 3H); ^{13}C NMR (100 MHz, $CDCl_3$): δ (ppm) 142.7, 139.6, 139.0, 137.9, 129.8, 128.7, 128.2, 128.0, 127.8, 121.7, 75.1, 21.0.

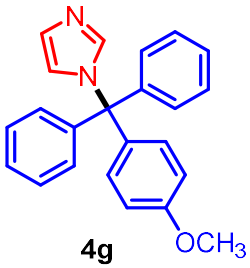

4g

1-((4-methoxyphenyl)diphenylmethyl)-1*H*-imidazole (4g): ^{1}H NMR (400 MHz, $CDCl_3$): δ (ppm) 7.37 (s, 1H), 7.27–7.18 (m, 6H), 7.12–7.01 (m, 4H), 7.00–6.95 (m, 3H), 6.79–6.70 (m, 3H), 3.72 (s, 3H); ^{13}C NMR (100 MHz, $CDCl_3$): δ (ppm) 159.1, 142.8, 139.0, 134.6, 131.2, 129.7, 128.2, 128.0, 121.7, 113.3, 74.9, 55.3.

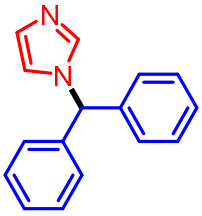

4h

1-benzhydryl-1*H*-imidazole (4h): ^{1}H NMR (400 MHz, $CDCl_3$): δ (ppm) 7.33 (d, J = 8.5 Hz, 1H), 7.32–7.23 (m, 6H), 7.03 (dd, J = 4.9, 2.7 Hz, 5H), 6.77 (s, 1H), 6.44 (s, 1H); ^{13}C NMR (100 MHz, $CDCl_3$): δ (ppm) 139.1, 137.4, 129.2, 128.9, 128.4, 128.1, 65.1.

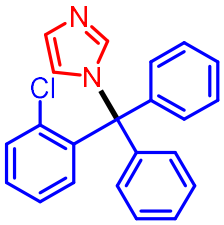

4i

1-((2-chlorophenyl)diphenylmethyl)-1*H*-imidazole (4i): ^{1}H NMR (400 MHz, $CDCl_3$): δ (ppm) 7.38 (s, 1H), 7.32 (dd, J = 7.8, 1.4 Hz, 1H), 7.26–7.20 (m, 7H), 7.18–7.07 (m, 5H), 6.96 (s, 1H), 6.84 (dd, J = 8.0, 1.6 Hz, 1H), 6.66 (s, 1H); ^{13}C NMR (100 MHz, $CDCl_3$): δ (ppm) 140.9, 140.4, 139.1, 135.6, 132.2, 130.4, 130.2, 129.9, 128.4, 128.2, 128.0, 127.0, 121.6, 75.1.

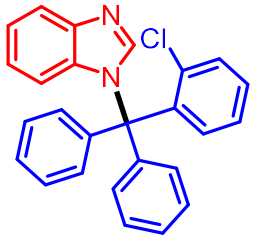

4j

1-((2-chlorophenyl)diphenylmethyl)-1*H*-benzo[d]imidazole (4j): ^{1}H NMR (400 MHz, $CDCl_3$): δ (ppm) 8.02 (s, 1H), 7.80 (d, J = 8.1 Hz, 1H), 7.44–7.14 (m, 15H), 6.95–6.86 (m, 1H), 6.45 (d, J = 8.3 Hz, 1H); ^{13}C NMR (100 MHz, $CDCl_3$): δ (ppm) 144.8, 144.5, 135.9, 134.6, 132.5, 131.4, 130.5, 129.9, 128.2, 128.1, 126.8, 122.5, 122.1, 120.3, 114.8, 75.6.

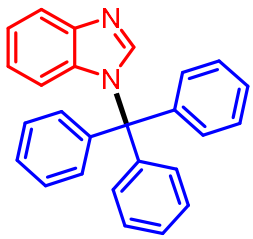

4k

1-trityl-1*H*-benzo[d]imidazole (4k): ^{1}H NMR (400 MHz, $CDCl_3$): δ (ppm) 7.92 (s, 1H), 7.81 (d, J = 8.1 Hz, 1H), 7.37–7.30 (m, 9H), 7.24–7.16 (m, 7H), 6.92 (t, J = 7.7 Hz, 1H), 6.50 (d, J = 8.3 Hz, 1H); ^{13}C NMR (100 MHz, $CDCl_3$): δ (ppm) 144.5, 144.1, 141.3, 134.7, 130.0, 128.2, 128.0, 122.4, 122.1, 120.2, 115.4, 75.5.

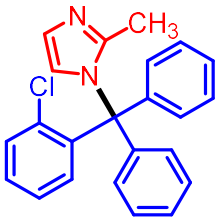

4l

1-((2-chlorophenyl)diphenylmethyl)-2-methyl-1*H*-imidazole (4l): ^{1}H NMR (400 MHz, $CDCl_3$): δ (ppm) 7.35 (dd, J = 7.8, 1.5 Hz, 1H), 7.29–7.17 (m, 8H), 7.06 (dd, J = 18.4, 5.6 Hz, 5H), 6.81 (d, J = 1.5 Hz, 1H), 6.74 (s, 1H), 1.49 (s, 3H); ^{13}C NMR (100 MHz, $CDCl_3$): δ (ppm) 146.8, 139.8, 135.8, 132.6, 130.8, 130.7, 129.8, 128.0, 127.8, 126.8, 124.9, 122.1, 75.2, 17.1.

^{1}H and ^{13}C NMR spectra of 1-methyl-3-trityl-1*H*-indole

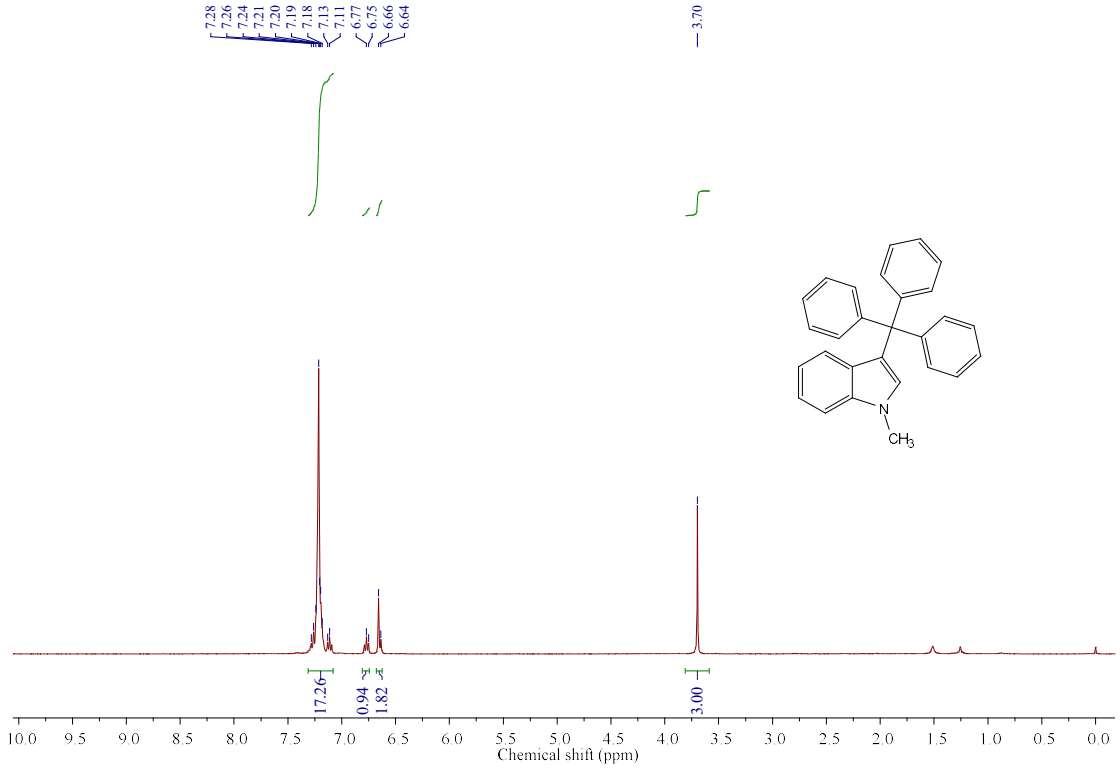

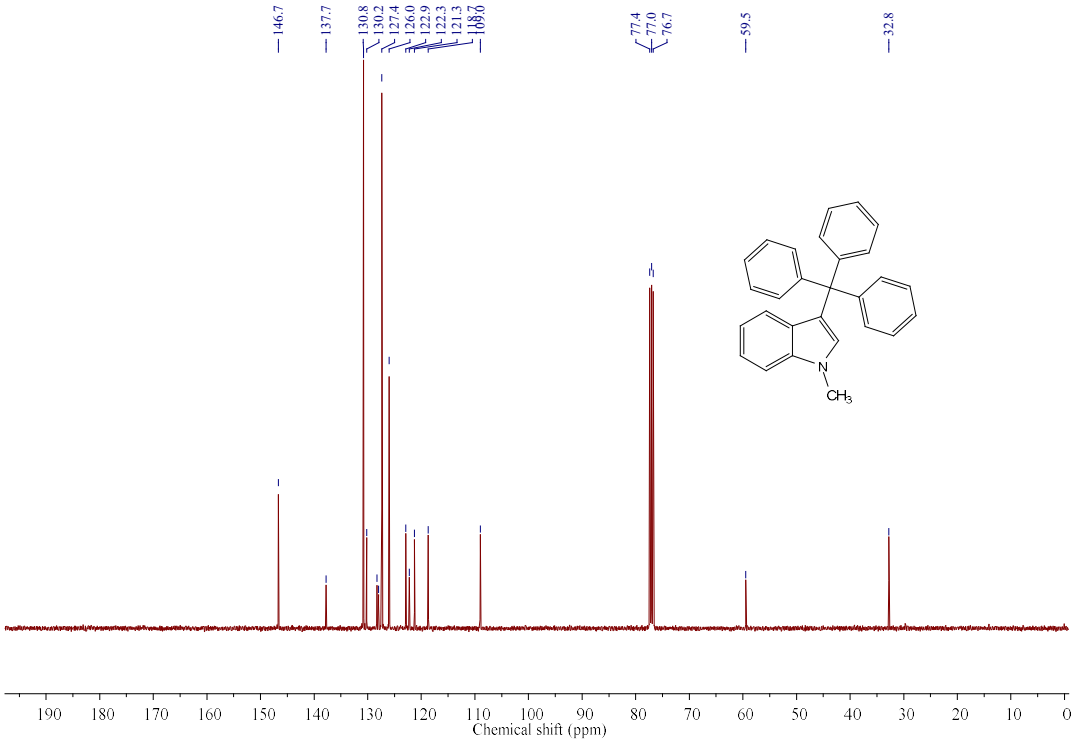

^{1}H and ^{13}C NMR spectra of 4-methyl-1-trityl-1*H*-imidazole

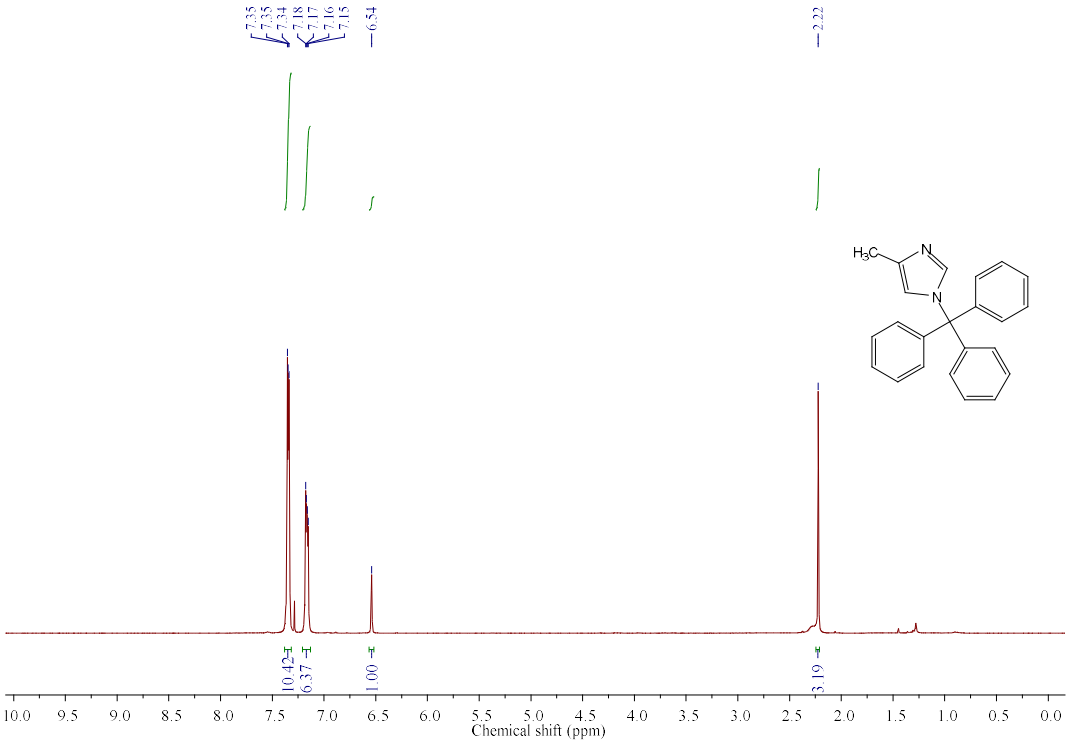

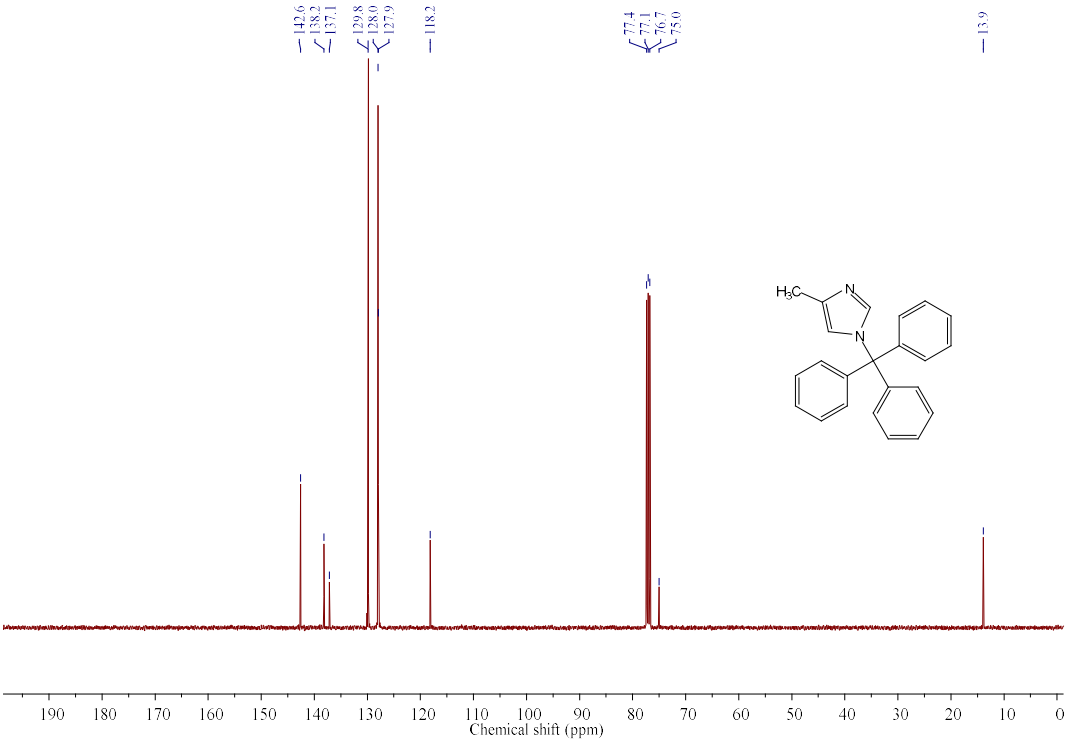

4.6 Bibliography

[1] Bains, A. K., Biswas, A., and Adhikari, D. Nickel-catalyzed chemoselective C-3 alkylation of indoles with alcohols through a borrowing hydrogen method. *Chemical Communications*, 56(98):15442-15445, 2020. (b) Bhattacharjee, P. and Bora, U. Molecular iodine-catalyzed selective C-3 benzylation of indoles with benzylic alcohols: a greener approach toward benzylated indoles. *ACS Omega*, 4(7):11770-11776, 2019. (c) Chakraborty, A., Debnath, S., Ghosh, T., Maiti, D. K., and Majumdar, S. An efficient strategy for *N*-alkylation of benzimidazoles/imidazoles in SDS-aqueous basic medium and *N*-alkylation induced ring opening of benzimidazoles. *Tetrahedron*, 74(40):5932-5941, 2018. (d) Karaaslan, C., Doganc, F., Alp, M., Koc, A., Karabay, A. Z., and Göker, H. Regioselective *N*-alkylation of some imidazole-containing heterocycles and their in vitro anticancer evaluation. *Journal of Molecular Structure*, 1205:127673, 2020. (e) Levi, L., Scheuren, S., and Mueller, T. J. A Novel *N*-Benzylation of Phenothiazine with Benzyl Alcohols Activated by n-Propylphosphonic Acid Anhydride (T3P®). *Synthesis*, 46(22):3059-3066, 2014. (f) Zhu, A., Feng, W., Li, L., Li, Q., and Wang, J. Hydroxyl functionalized Lewis acidic ionic liquid on silica: an efficient catalyst for the C-3 Friedel-Crafts benzylation of indoles with benzyl alcohols. *Catalysis Letters*, 147(1):261-268, 2017.

[2] Shiri, M. Indoles in multicomponent processes (MCPs). *Chemical Reviews*, 112(6):3508-3549, 2012.

[3] Homer, J. A. and Sperry, J. Mushroom-derived indole alkaloids. *Journal of Natural Products*, 80(7):2178-2187, 2017.

[4] (a) Hikawa, H., Suzuki, H., and Azumaya, I. Au(III)/TPPMS-catalyzed benzylation of indoles with benzylic alcohols in water. *The Journal of Organic Chemistry*, 78(23):12128-12135, 2013. (b) Siddiki, S. H., Kon, K., and Shimizu, K. I. General and Selective C-3 Alkylation of Indoles with Primary Alcohols by a Reusable Pt Nanocluster Catalyst. *Chemistry–A European Journal*, 19(43):14416-14419, 2013. (c) Koller, S., Blazejak, M., and Hintermann, L. Catalytic C-Alkylation of Pyrroles with Primary Alcohols: Hans Fischer's Alkali and a New Method with Iridium P, N, P-Pincer Complexes. *European Journal of Organic Chemistry*, 2018(14):1624-1633, 2018.

(d) Bähn, S., Imm, S., Mevius, K., Neubert, L., Tillack, A., Williams, J. M., and Beller, M. Selective Ruthenium-Catalyzed *N*-Alkylation of Indoles by Using Alcohols. *Chemistry–A European Journal*, 16(12):3590-3593, 2010.

[5] (a) Rueping, M. and Nachtsheim, B. J. A review of new developments in the Friedel–Crafts alkylation–From green chemistry to asymmetric catalysis. *Beilstein Journal of Organic Chemistry*, 6(1):6, 2010. (b) Herrera, R. P., Sgarzani, V., Bernardi, L., and Ricci, A. Catalytic enantioselective Friedel–Crafts alkylation of indoles with nitroalkenes by using a simple thiourea organocatalyst. *Angewandte Chemie*, 117(40):6734-6737, 2005.

[6] Yu, L., Li, S. S., Li, W., Yu, S., Liu, Q., and Xiao, J. Fluorinated Alcohol-Promoted Reaction of Chlorohydrocarbons with Diverse Nucleophiles for the Synthesis of Triarylmethanes and Tetraarylmethanes. *The Journal of Organic Chemistry*, 83(24):15277-15283, 2018.

[7] (a) Tonelli, M., Simone, M., Tasso, B., Novelli, F., Boido, V., Sparatore, F., Paglietti, G., Pricl, S., Giliberti, G., Blois, S., and Ibba, C. Antiviral activity of benzimidazole derivatives. II. Antiviral activity of 2-phenylbenzimidazole derivatives. *Bioorganic & Medicinal Chemistry*, 18(8):2937-2953, 2010. (b) Shaharyar, M., Abdullah, M. M., Bakht, M. A., and Majeed, J. Pyrazoline bearing benzimidazoles: Search for anticancer agent. *European Journal of Medicinal Chemistry*, 45(1):114-119, 2010.

[8] Bie, F., Yao, Y., Cao, H., Shi, Y., Yan, P., Ma, J., Han, Y., and Liu, X. Convenient synthesis of N-1-alkyl benzimidazoles *via* Pd catalyzed C–N bond formation and cyclization. *Synthetic Communications*, 51(15):2387-2396, 2021.

[9] (a) Vu, P. D., Boydston, A. J., and Bielawski, C. W. Ionic liquids *via* efficient, solvent-free anion metathesis. *Green Chemistry*, 9(11):1158-1159, 2007. (b) Deetlefs, M. and Seddon, K. R. Improved preparations of ionic liquids using microwave irradiation. *Green Chemistry*, 5(2):181-186, 2003. (c) Varma, R. S. and Namboodiri, V. V. An expeditious solvent-free route to ionic liquids using microwaves. *Chemical Communications*, (7):643-644, 2001.

[10] Yadav, J. S., Reddy, B. S., and Reddy, A. S. Phosphomolybdic acid-supported silica gel as efficient and cost-effective solid acid for the benzylation of indoles with benzylic alcohols. *Journal of Molecular Catalysis A: Chemical*, 280(1-2):219-223, 2008.

[11] Nair, V., Thomas, S., Mathew, S. C., and Abhilash, K. G. Recent advances in the chemistry of triaryl-and triheteroarylmethanes. *Tetrahedron*, 29(62):6731-6747, 2006.

[12] Shchepinov, M. S. and Korshun, V. A. Recent applications of bifunctional trityl groups. *Chemical Society Reviews*, 32(3):170-180, 2003.

[13] (a) Cavallo, G., Metrangolo, P., Milani, R., Pilati, T., Priimagi, A., Resnati, G., and Terraneo, G. The halogen bond. *Chemical Reviews*, 116(4):2478-2601, 2016. (b) Sutar, R. L. and Huber, S. M. Catalysis of organic reactions through halogen bonding. *ACS Catalysis*, 9(10):9622-9639, 2019.

[14] (a) Nandy, A., Kazi, I., Guha, S., and Sekar, G. Visible-light-driven halogen-bond-assisted direct synthesis of heteroaryl thioethers using transition metal-free one-pot C–I bond formation/C–S cross-coupling reaction. *The Journal of Organic Chemistry*, 86(3):2570-2581, 2021. (b) Kazi, I., Guha, S., and Sekar, G. Halogen bond-assisted electron-catalyzed atom economic iodination of heteroarenes at room temperature. *The Journal of Organic Chemistry*, 84(11):6642-6654, 2019.

[15] (a) Politzer, P., Lane, P., Concha, M. C., Ma, Y., and Murray, J. S. An overview of halogen bonding. *Journal of Molecular Modeling*, 13(2):305-311, 2007. (b) Carlsson, A. C. C., Uhrbom, M., Karim, A., Brath, U., Gräfenstein, J., and Erdélyi, M. Solvent effects on halogen bond symmetry. *CrystEngComm*, 15(16):3087-3092, 2013. (c) Forni, A., Rendine, S., Pieraccini, S., and Sironi, M. Solvent effect on halogen bonding: The case of the I···O interaction. *Journal of Molecular Graphics and Modelling*, 38:31-39, 2012. (d) Metrangolo, P., Neukirch, H., Pilati, T., and Resnati, G. Halogen bonding based recognition processes: a world parallel to hydrogen bonding. *Accounts of Chemical Research*, 38(5):386-395, 2005. (e) Sarwar, M. G., Ajami, D., Theodorakopoulos, G., Petsalakis, I. D., and Rebek Jr, J. Amplified halogen bonding in a small space. *Journal of the American Chemical Society*, 135(37):13672-13675, 2013. (f) Pan, F., Dashti, M., Reynolds, M. R., Rissanen, K., Trant, J. F., and Beyeh, N. K. Halogen bonding and host–guest chemistry between N-alkylammonium resorcinarene halides, diiodoperfluorobutane and neutral guests. *Beilstein Journal of Organic Chemistry*, 15(1):947-954, 2019. (g) Pearcy, A. C., Mason, K. A., and El-Shall, M. S. Ionic hydrogen and halogen bonding in the gas phase association of

acetonitrile and acetone with halogenated benzene cations. *The Journal of Physical Chemistry A*, 123(7):1363-1371, 2018. (h) Gao, X., Chang, R., Rao, J., Hao, D., Zhang, Z., Zhou, C. Y., and Guo, Z. Halogen-Bonding-Promoted C–H Malonylation of Indoles under Visible-Light Irradiation. *The Journal of Organic Chemistry*, 87(12):8198-8202, 2022.

[16] Varadwaj, P. R., Varadwaj, A., and Jin, B. Y. Halogen bonding interaction of chloromethane with several nitrogen donating molecules: Addressing the nature of the chlorine surface σ-hole. *Physical Chemistry Chemical Physics*, 16(36):19573-19589, 2014.

[17] Kollman, P. Non-covalent forces of importance in biochemistry. In *New Comprehensive Biochemistry*, pages 55-71, Elsevier, 1984.

[18] (a) Tawfik, M. and Donald, K. J. Halogen bonding: unifying perspectives on organic and inorganic cases. *The Journal of Physical Chemistry A*, 118(43):10090-10100, 2014. (b) Auffinger, P., Hays, F. A., Westhof, E., and Ho, P. S. Halogen bonds in biological molecules. *Proceedings of the National Academy of Sciences*, 101(48):16789-16794, 2004. (c) De Moliner, E., Brown, N. R., and Johnson, L. N. Alternative binding modes of an inhibitor to two different kinases. *European Journal of Biochemistry*, 270(15):3174-3181, 2003. (d) Metrangolo, P., Pilati, T., Resnati, G., and Stevenazzi, A. Halogen bonding driven self-assembly of fluorocarbons and hydrocarbons. *Current Opinion in Colloid & Interface Science*, 8(3):215-222, 2003. (e) Palusiak, M. On the nature of halogen bond–The Kohn–Sham molecular orbital approach. *Journal of Molecular Structure: THEOCHEM*, 945(1-3):89-92, 2010.

[19] Das, D. and Roy, S. Palladium(II)-Catalyzed Efficient C-3 Functionalization of Indoles with Benzylic and Allylic Alcohols under Co-Catalyst, Acid, Base, Additive and External Ligand-Free Conditions. *Advanced Synthesis & Catalysis*, 355(7):1308-1314, 2013.

[20] Politzer, P., Murray, J. S., and Clark, T. Halogen bonding: an electrostatically-driven highly directional non-covalent interaction. *Physical Chemistry Chemical Physics*, 12(28):7748-7757, 2010.

[21] Matuszak, C. A. and Matuszak, A. J. Imidazole-versatile today, prominent tomorrow. *Journal of Chemical Education*, 53(5):280, 1976.

[22] Erdelyi, M. Halogen bonding in solution. *Chemical Society Reviews*, 41(9):3547-3557, 2012.

[23] Hawthorne, B., Fan-Hagenstein, H., Wood, E., Smith, J., and Hanks, T. Study of the halogen bonding between pyridine and perfluoroalkyl iodide in solution phase using the combination of FT-IR and ^{19}F NMR. *International Journal of Spectroscopy*, 2013, 2013.

[24] Riley, K. E. and Hobza, P. Investigations into the nature of halogen bonding including symmetry adapted perturbation theory analyses. *Journal of Chemical Theory and Computation*, 4(2):232-242, 2008.